Conjugated turbulent heat transfer with axial conduction in wall and convection boundary conditions in a parallel-plate channel

R. O. C. Guedes and M. N. Özişik
Mechanical and Aerospace Engineering Department, North Carolina State University, Raleigh, NC, USA

The steady-state conjugated turbulent heat transfer with axial conduction in the wall and convection boundary conditions is solved with the generalized integral transform technique for the flow of Newtonian fluid in a parallel-plate duct. A lumped wall model that neglects transverse temperature gradients in the solid but that takes into account the axial heat conduction along the wall is adopted. Highly accurate results are presented for the fluid bulk and wall temperatures and Nusselt number. The effects of the conjugation parameter, Biot number, and the dimensionless channel length on Nusselt number and fluid bulk and wall temperatures are systematically investigated.

Keywords: generalized integral transform technique; thermal entry region

Introduction

In the studies of heat transfer for forced convection inside ducts, it is common practice to impose temperature or heat-flux boundary conditions at the fluid–solid interface, as in the case of classical Graetz problem, which neglects the participation of the duct wall in the heat transfer process. In most physically realistic situations, however, the boundary conditions at the interface are not known a priori, but depend on the coupled conduction–convection mechanism. As pointed out in recent reviews (Shah and London 1978; Shah and Bhatti 1987), the inclusion of wall conduction may have a significant effect on heat transfer, especially in the thermal entrance region. This is important in heat-exchanger theory and applications.

Most of the available work on conjugated heat transfer has been on laminar flow. Approximate analytical solutions (Luikov et al. 1971; Mori et al. 1976) demonstrate the mathematical difficulties associated with the solution of such problems. Seminumerical approaches (Barrozi and Pagliarini 1985) and purely numerical approaches (Campo and Schuler 1988) illustrate the computational involvement in dealing with coupled convection–conduction systems. On the other hand, a simple model that lumps the tube wall temperature in the radial direction but retains the axial conduction along the wall was used by Faghri and Sparrow (1980), Zariffeh et al. (1982), and Wijeysundera (1986).

In the case of turbulent conjugated heat transfer in ducts, the problem is far more involved and has not received much attention. The few analytical studies available (Sakakibara and Endoh 1977; Lin and Chow 1984) use Duhamel's theorem together with a polynomial representation of interfacial temperature to solve the problem. Numerical approaches (Yan et al. 1990) use the finite-difference technique with nonuniform grids.

Address reprint requests to Professor Özişik at the Mechanical and Aerospace Engineering Department, North Carolina State University, Raleigh, NC 27695, USA.

Received 23 September 1991; accepted 19 April 1992

In the present work, we consider steady-state conjugated turbulent flow with convection boundary conditions by lumping the wall in the radial direction while retaining the axial conduction along the duct wall. To solve this problem analytically, the ideas in the generalized integral transform technique (Ozisik and Murray 1974; Cotta and Ozisik 1986, 1987; Ozisik et al. 1989; Guedes et al. 1991) are extended to handle the more general type of boundary condition encountered in the wall lumping procedure.

Analysis

Steady-state heat transfer to hydrodynamically developed, thermally developing turbulent flow of an incompressible Newtonian fluid inside a smooth, parallel-plate channel is considered by allowing for the conjugation between the fluid and the duct wall. Under the assumptions of constant properties and negligible viscous dissipation and fluid axial conduction effects, the mathematical formulation of the problem in dimensionless form is given as follows:

Solid region

$$\frac{\partial^2 \Theta_s(R,Z)}{\partial Z^2} + \frac{C^2\,\mathrm{Pe}^2}{16}\frac{\partial^2 \Theta_s(R,Z)}{\partial R^2} = 0,\ 1 < R < \delta,\ 0 < Z < L \quad (1a)$$

with boundary conditions

$$\frac{\partial \Theta_s(R,0)}{\partial Z} = 0,\ 1 \leqslant R \leqslant \delta \quad (1b)$$

$$\frac{\partial \Theta_s(R,L)}{\partial Z} = 0,\ 1 \leqslant R \leqslant \delta \quad (1c)$$

$$\frac{\partial \Theta_s(\delta,Z)}{\partial R} + \bar{\mathrm{Bi}}\,\Theta_s(\delta,Z) = 0,\ Z > 0 \quad (1d)$$

Fluid region

$$W(R)\frac{\partial \Theta_f(R,Z)}{\partial Z} = \frac{\partial}{\partial R}\left(\varepsilon(R)\frac{\partial \Theta_f(R,Z)}{\partial R}\right),\ 0 < R < 1\ \ Z > 0 \quad (2a)$$

with inlet and boundary conditions

$$\Theta_f(R, 0) = 1, \quad 0 \leqslant R \leqslant 1 \tag{2b}$$

$$\frac{\partial \Theta_f(0, Z)}{\partial R} = 0, \qquad Z > 0 \tag{2c}$$

and the continuity of temperature and heat flux at the solid–fluid interface

$$\Theta_f(1, Z) = \Theta_s(1, Z), \qquad 0 \leqslant Z \leqslant L \tag{3a}$$

$$K_{fs} \frac{\partial \Theta_f(1, Z)}{\partial R} = \frac{\partial \Theta_s(1, Z)}{\partial R}, \qquad 0 \leqslant Z \leqslant L \tag{3b}$$

where the various dimensionless quantities are defined in the nomenclature. The models for turbulent velocity distribution and eddy diffusivity are given in Appendix 1. The determination of the coefficient C, which represents the ratio of the maximum velocity to the mean velocity, is given in Appendix 2.

The analytical solution of the above system is quite an involved matter; to simplify the analysis, the axial conduction along the wall is retained, but the transverse wall conduction is lumped by operating on the wall energy equation (Equation 1a) with the operator $\int_1^\delta (dR/\delta - 1)$. Equation 1a reduces to

$$\frac{d^2\Theta_{sm}(Z)}{dZ^2} + \frac{C^2\,\mathrm{Pe}^2}{16(\delta - 1)}\left(\frac{\partial \Theta_s(\delta, Z)}{\partial R} - \frac{\partial \Theta_s(1, Z)}{\partial R}\right) = 0 \tag{4a}$$

where the average wall temperature is defined as

$$\Theta_{sm}(Z) = \frac{1}{\delta - 1}\int_1^\delta \Theta_s(R, Z)\, dR \tag{4b}$$

and the derivative terms appearing inside the bracket in Equation 4a are eliminated by utilizing the boundary conditions (Equations 1d and 3b) to yield:

$$\frac{d^2\Theta_{sm}(Z)}{dZ^2} - \frac{C^2\,\mathrm{Pe}^2}{16(\delta - 1)}\left(\bar{\mathrm{Bi}}\,\Theta_s(\delta, Z) + K_{fs}\frac{\partial \Theta_f(1, Z)}{\partial R}\right) = 0 \tag{5}$$

Furthermore, under the assumption of negligible transverse temperature gradients within the wall, we have

$$\Theta_{sm}(Z) \approx \Theta_s(\delta, Z) \approx \Theta_s(1, Z) \tag{6}$$

Now, utilizing Equation 6 together with the interface condition (Equation 3a) in Equation 5, we obtain

$$\frac{\partial \Theta_f(1, Z)}{\partial R} + \mathrm{Bi}\,\Theta_f(1, Z) = \beta \frac{\partial^2 \Theta_f(1, Z)}{\partial Z^2} \tag{7a}$$

where

$$\mathrm{Bi} = \frac{\bar{\mathrm{Bi}}}{K_{fs}} \tag{7b}$$

$$\beta = \frac{16(\delta - 1)}{C^2\,\mathrm{Pe}^2\,K_{fs}} \tag{7c}$$

Thus, the original heat conduction (Equation 1a) for the wall is now transformed to a boundary condition given by Equation 7a for use in the fluid energy equation (Equation 2a) at $R = 1$. Here, the conjugation parameter, β, is introduced in order to incorporate the effects of several different factors on heat transfer into a single parameter. The limiting case of $\beta \to 0$ represents negligible wall conjugation effects, which corresponds to the classical Graetz problem with a convection boundary condition.

To solve the problem given by Equations 2a–2c and Equation 7a simultaneously by using an analytic approach, the ideas in the generalized integral transform technique are extended as described below.

Notation

Bi	Fluid Biot number ($h_\infty r_1/K_f$)
$\bar{\mathrm{Bi}}$	Wall Biot number ($h_\infty r_1/K_s$)
C	Maximum to mean velocity ratio ($u_{max}/\bar{u}$)
c_p	Specific heat of the fluid
D_e	equivalent diameter ($4r_1$)
E	Constant defined in Appendix 1
f_m	Friction factor
$h(z)$	Convective heat transfer coefficient (internal) computed from the present analysis
h_∞	Ambient convective heat transfer coefficient
K_s, K_f	Thermal conductivities of solid and fluid, respectively
k	Constant appearing in Appendix 1
K_{fs}	Thermal conductivity ratio (K_f/K_s)
L^*	Length of heat transfer section, dimensional
L	Length of heat transfer section, dimensionless ($16L^*\,\alpha_f/C\bar{u}D_e^2$)
$\mathrm{Nu}(z)$	Local Nusselt number ($h(z)D_e/K_f$)
Pe	Peclet number ($\bar{u}D_e/\alpha_f$)
Pr	Prandtl number (ν/α)
Re	Reynolds number ($\bar{u}D_e/\nu$)
r_1, r_2	Distance of the inner and outer surfaces of the wall from the centerline (dimensional), respectively
r	Transverse coordinate (dimensional)
r^+	Parameter defined in Appendix 1
R	Transverse coordinate (dimensionless) (r/r_1)
T_∞, T_0	Ambient and inlet temperatures, respectively
$T_s(r, z)$	Solid temperature
$T_f(r, z)$	Fluid temperature
u^+	Turbulent velocity defined in Appendix 1
$\bar{u}$	Average flow velocity
u_{max}	Maximum flow velocity
$u(r)$	Velocity distribution (dimensional)
$W(R)$	Velocity distribution (dimensionless) ($u(r)/C\bar{u}$)
$\mathbf{y}(Z)$	Vector of unknowns defined by Equation 17b
z	Axial coordinate (dimensional)
Z	Axial coordinate (dimensionless) ($16z\alpha_f/C\bar{u}D_e^2$)

Greek symbols

α_f	Thermal diffusivity of the fluid
β	Conjugation parameter (dimensionless), defined by Equation 7c
δ	Aspect ratio (r_2/r_1)
$\varepsilon(R)$	Dimensionless total diffusivity ($1 + \varepsilon_h/\alpha_f$)
ε_h	Eddy diffusivity for heat
ε_m	Eddy diffusivity for momentum
$\Theta(R, Z)$	Dimensionless fluid temperature distribution ($[T(r, z) - T_\infty]/[T_0 - T_\infty]$)
$\Theta_{av}(Z)$	Dimensionless average (bulk) temperature, defined by Equation 11b
μ_i	Eigenvalues of Sturm–Liouville problem (Equations 8a-8c)
$\psi(\mu_i, R)$	Eigenfunctions of Sturm–Liouville problem (Equations 8a-8c)
ν	Kinematic viscosity

First, we consider the following standard auxiliary eigenvalue problem:

$$\frac{d}{dR}\left(\varepsilon(R)\frac{d\psi(\mu_i,R)}{dR}\right)+\mu_i^2 W(R)\psi(\mu_i,R)=0, \quad 0<R<1 \tag{8a}$$

$$\frac{d\psi(\mu_i,R)}{dR}=0, \qquad R=0 \tag{8b}$$

$$\frac{d\psi(\mu_i,R)}{dR}+\mathrm{Bi}\,\psi(\mu_i,R)=0, \qquad R=1 \tag{8c}$$

Then, by utilizing the eigenfunctions of this system, we define the integral transform pair as

$$\Theta_f(R,Z)=\sum_{i=1}^{\infty}\frac{\psi(\mu_i,R)}{N_i^{1/2}}\bar{\Theta}_i(Z), \qquad \text{inversion} \tag{9a}$$

$$\bar{\Theta}_i(Z)=\int_0^1 W(R)\frac{\psi(\mu_i,R)}{N_i^{1/2}}\Theta_f(R,Z)\,dR, \qquad \text{transform} \tag{9b}$$

where the normalization integral is given by

$$N_i=\int_0^1 W(R)[\psi(\mu_i,R)]^2\,dR \tag{9c}$$

Following the formalism in the generalized integral transform technique, the fluid energy equation (Equation 2a) is operated on by the operator

$$\int_0^1\frac{\psi(\mu_i,R)}{N_i^{1/2}}\,dR$$

to obtain

$$\frac{d\bar{\Theta}_i(Z)}{dZ}+\mu_i^2\bar{\Theta}_i(Z)=\frac{1}{N_i^{1/2}}\times\left[\psi(\mu_i,1)\frac{\partial\Theta_f(1,Z)}{\partial R}-\Theta_f(1,Z)\frac{\partial\psi(\mu_i,1)}{\partial R}\right] \tag{10a}$$

The terms inside the bracket on the right-hand side of Equation 10a are evaluated in the following manner: Equation 8c is multiplied by $\Theta_f(1,Z)$, and Equation 7a by $\psi(\mu_i,1)$, and the results are subtracted to yield

$$\left[\psi(\mu_i,1)\frac{\partial\Theta_f(1,Z)}{\partial R}-\Theta_f(1,Z)\frac{\partial\psi(\mu_i,1)}{\partial R}\right]=\beta\psi(\mu_i,1)\frac{\partial^2\Theta_f(1,Z)}{\partial Z^2} \tag{10b}$$

Introducing this result into Equation 10a, we obtain

$$\frac{d\bar{\Theta}_i(Z)}{dZ}+\mu_i^2\bar{\Theta}_i(Z)=\frac{\beta}{N_i^{1/2}}\psi(\mu_i,1)\frac{\partial^2\Theta_f(1,Z)}{\partial Z^2} \quad i=1,2,\ldots \tag{10c}$$

Equation 10c contains two unknowns, $\bar{\Theta}_i(Z)$ and $\Theta_f(1,Z)$. An expression can be developed for the latter by integrating the fluid energy equation (Equation 2a) over the duct cross section to yield

$$\frac{d\Theta_{av}(Z)}{dZ}=C\frac{\partial\Theta_f(1,Z)}{\partial R} \tag{11a}$$

where the fluid bulk temperature is defined as

$$\Theta_{av}(Z)=C\int_0^1 W(R)\Theta_f(R,Z)\,dR \tag{11b}$$

By replacing $\Theta_f(R,Z)$ by its equivalent inversion formula, given by Equation 9a, Equation 11b takes the form

$$\Theta_{av}(Z)=C\sum_{i=1}^{\infty}\bar{f}_i\bar{\Theta}_i(Z), \tag{11c}$$

where $\bar{f}_i$ is defined as

$$\bar{f}_i=\int_0^1 W(R)\frac{\psi(\mu_i,R)}{N_i^{1/2}}\,dR \tag{11d}$$

Now, utilizing Equations 11a and 11c, the term $\partial\Theta_f(1,Z)/\partial R$ in Equation 7a is eliminated. Then Equation 7a takes the form

$$\beta\frac{d^2\Theta_w(Z)}{dZ^2}-\mathrm{Bi}\,\Theta_w(Z)=\sum_{j=1}^{\infty}\bar{f}_j\frac{d\bar{\Theta}_j(Z)}{dZ} \tag{12}$$

where the notation $\Theta_w(Z)\equiv\Theta_f(1,Z)$ is introduced for simplicity. Equations 10c and 12 provide two relations for the determination of the two unknowns, $\Theta_w(Z)$ and $\bar{\Theta}_i(Z)$. Substituting Equation 12 into Equation 10c, the second derivative term is eliminated. Then, the following system of coupled differential equations is obtained:

$$\sum_{j=1}^{\infty}a_{ij}\frac{d\bar{\Theta}_j(Z)}{dZ}+\mu_i^2\bar{\Theta}_i(Z)=\mathrm{Bi}\frac{\psi(\mu_i,1)}{N_i^{1/2}}\Theta_w(Z), i=1,2,\ldots \tag{13a}$$

which is written in the matrix form as

$$\mathbf{A}\bar{\Theta}'(Z)+\mathbf{D}\bar{\Theta}(Z)=\Theta_w(Z)\mathbf{g} \tag{13b}$$

where the prime denotes the derivative with respect to Z, and various quantities are defined as

$$\mathbf{A}=\{a_{ij}\},\ a_{ij}=\delta_{ij}-\frac{\psi(\mu_i,1)}{N_i^{1/2}}\bar{f}_j \tag{13c}$$

$$\mathbf{D}=\{d_{ij}\},\ d_{ij}=\delta_{ij}\mu_i^2 \tag{13d}$$

$$\mathbf{g}=\{g_i\}^t,\ g_i=\mathrm{Bi}\frac{\psi(\mu_i,1)}{N_i^{1/2}} \tag{13e}$$

with

$$\delta_{ij}=\begin{cases}0 & i\neq j\\ 1 & i=j\end{cases} \tag{13f}$$

System 13b is now rearranged in the form

$$\frac{d\bar{\Theta}_i(Z)}{dZ}+\sum_{j=1}^{\infty}e_{ij}\bar{\Theta}_j(Z)=h_i\Theta_w(Z),\ i=1,2,\ldots \tag{14a}$$

where

$$\mathbf{E}=\{e_{ij}\},\ \mathbf{E}=\mathbf{A}^{-1}\mathbf{D} \tag{14b}$$

$$\mathbf{h}=\{h_i\}^t,\ \mathbf{h}=\mathbf{A}^{-1}\mathbf{g} \tag{14c}$$

and the superscript t denotes the transpose. Equation 14a is introduced in Equation 12 in order to eliminate the first derivative $d\bar{\Theta}_j(Z)/dZ$, yielding

$$\beta\frac{d^2\Theta_w(Z)}{dZ^2}-\left(\mathrm{Bi}+\sum_{k=1}^{\infty}\bar{f}_k h_k\right)\Theta_w(Z)=-\sum_{j=1}^{\infty}\left(\sum_{k=1}^{\infty}\bar{f}_k e_{kj}\right)\bar{\Theta}_j(Z) \tag{15}$$

Thus, Equations 14a and 15 are the two coupled equations for the determination of the unknowns $\Theta_w(Z)$ and $\bar{\Theta}_j(Z)$. The boundary conditions for this system are given by

$$\bar{\Theta}_i(0)=\bar{f}_i,\ i=1,2,\ldots \tag{16a}$$

$$\frac{d\Theta_w(0)}{dZ}=0 \tag{16b}$$

$$\frac{d\Theta_w(L)}{dZ}=0 \tag{16c}$$

Equations 14a and 15 are rewritten in matrix form. After truncating the infinite sums at a sufficiently large-order N, the

resulting system of $N + 2$ coupled ordinary differential equations is written in the matrix form as

$$\mathbf{y}'(Z) = \mathbf{B}\mathbf{y}(Z) \tag{17a}$$

where

$$\mathbf{y} = \{\bar{\Theta}_1(Z), \ldots, \bar{\Theta}_N(Z), \Theta_w(Z), \Theta'_w(Z)\}^t \tag{17b}$$

and the $(N + 2) \times (N + 2)$ elements b_{ij} of matrix $\mathbf{B}$ are given by

Elements	Range of i	Range of j
$-e_{ij}$	$i \leqslant N$	$j \leqslant N$
h_i	$i \leqslant N$	$j = N + 1$
0	$i \leqslant N$	$j = N + 2$
$\delta_{j,N+2}$	$i = N + 1$	$j \leqslant N + 2$
$-\frac{1}{\beta}\left(\sum_{k=1}^{N} \bar{f}_k e_{kj}\right)$	$i = N + 2$	$j \leqslant N$
$\frac{1}{\beta}\left(\mathrm{Bi} + \sum_{k=1}^{N} \bar{f}_k\right)$	$i = N + 2$	$j = N + 1$
0	$i = N + 2$	$j = N + 2$

(17c)

Equation 17a provides a system of equations for the solution vector, $\mathbf{y}(Z)$. The eigenvalues, λ's, and eigenvectors, ξ's, of matrix $\mathbf{B}$ are determined by the solution of the following algebraic problem:

$$(\mathbf{B} - \lambda\mathbf{I})\xi = \mathbf{0} \tag{18a}$$

The solution for $\mathbf{y}(Z)$ is then constructed as

$$\mathbf{y}(Z) = \sum_{j=1}^{N+2} c_j \xi(j) e^{\lambda_j Z} \tag{18b}$$

where the constants c_j's are computed by constraining the solution $\mathbf{y}(Z)$ to satisfy the boundary conditions given by Equations 16a–16c. The following linear system of algebraic equations result for the determination of the constants c_j:

$$\begin{aligned} &\sum_{j=1}^{N+2} c_j \xi_i(j) = \bar{f}_i \qquad i = 1, 2, \ldots, N \\ &\sum_{j=1}^{N+2} c_j \lambda_j \xi_{N+1}(j) = 0 \\ &\sum_{j=1}^{N+2} c_j \lambda_j \xi_{N+1}(j) e^{\lambda_j L} = 0 \end{aligned} \tag{18c}$$

Both Equations 18a and 18c are readily solved through advanced scientific subroutine packages, such as the IMSL library (1987).

Once the vector $\mathbf{y}(Z)$ has been obtained, the inversion formula (Equation 9a) is applied to construct the solution for the original fluid temperature field, $\Theta_f(R, Z)$, while the lumped wall temperature, $\Theta_w(Z)$, is obtained directly from the $(N + 1)$th element of solution vector $\mathbf{y}(Z)$.

Also of interest is the local Nusselt number, which is obtained from its definition given by

$$\mathrm{Nu}(Z) = \frac{h(z)D_e}{K_f} = \frac{4[\partial\Theta_w(Z)/\partial R]}{\Theta_w(Z) - \Theta_{av}(Z)} \tag{19}$$

Results and discussion

Numerical computations are performed to study the effects of the conjugation parameter β and the Biot, Prandtl, and Reynolds numbers on the wall and bulk temperatures and on the local Nusselt number $\mathrm{Nu}(Z)$. The eigenvalue problem defined by Equation 18a was solved by the IMSL subroutine DEVCRG, while the linear system of algebraic equations (Equations 18c) was solved by the IMSL subroutine DLSACG. The number of eigenvalues needed for a specified convergence depends on the Reynolds, Prandtl, and Biot numbers and the location along the channel. In all the cases studied here, $N = 60$ terms ensured convergence of at least four significant digits over a wide range of parameters, including axial dimensionless distance Z (10^{-5} to 10), Reynolds number (10^4 to 10^5), Prandtl number (10^{-2} to 10^0), and Biot number (10^0 to 10^2). With the present method of analysis, as many eigenvalues as needed could be determined with no difficulty. From practical considerations, the values for the conjugation parameter studied ranged from $\beta = 10^{-8}$ to $\beta = 10^{-3}$. The case $\beta = 0$ corresponds to the classical Graetz problem for turbulent flow with a convective boundary condition, but no conjugation.

Figures 1a, 1b, 1c show the variation of wall temperature distribution along the duct for three different Biot numbers—1, 10, and 100, respectively—while fixing the values of other parameters as $\mathrm{Pr} = 0.72$, $\mathrm{Re} = 10^4$, and $L = 10$. Increasing β, the temperature distribution along the wall is progressively flattened, and an asymptotic value is attained in the region close to the inlet. For the limiting case of $\beta \to \infty$, the problem reduces to the turbulent Graetz problem with uniform prescribed wall temperature boundary condition. Figures 1a, 1b, and 1c also reveal that increasing the Biot number decreases the peak temperature. For axial distances far away from the inlet, the temperature gradients along the wall become small enough to cause the conjugation effects to disappear and the curves for different values of β join the curve for no conjugation. The wall conduction causes a fin effect that carries heat away to downstream regions with little temperature gradients. Similar trends are obtained for other combinations of Re and Pr, although the effects are less significant for higher Reynolds numbers. For fixed Pr and Re numbers, other values of L should not affect the above trends significantly.

Figure 2 shows that the fluid bulk temperature remains unaffected by the variation of the conjugation parameter from $\beta = 0$ to $\beta = 10^{-3}$. The same trend is observed for all other combinations of Bi, Re, and Pr in the ranges stated above. The flattening of the wall temperature near the entrance is caused by increased heat losses to the wall. On the other hand, heat losses through the walls being only a small fraction of the total heat carried by the bulk fluid, the temperature of the bulk fluid remains essentially unaffected by the increased heat losses of the wall.

Figures 3a and 3b show the effects of the conjugation parameter on the local Nusselt numbers for the two extreme cases $\mathrm{Bi} = 1$ and 100 considered here, respectively. Decreasing β increase the local Nusselt number near the inlet region. As β approaches zero, the local Nusselt number approaches that for the Graetz problem with convective boundary condition. The conjugation effects become less significant for higher Re and Pr. On the other hand, decreasing Pr increases the deviation of the local Nusselt number from that for the Graetz problem.

The difference between the local Nusselt numbers calculated with and without conjugation effects (the Graetz problem with convective boundary condition) for some Pr numbers is illustrated in Table 1 for the case of $\mathrm{Bi} = 1$, while Table 2 shows similar results for the case of $\mathrm{Bi} = 10$. Since the dimensionless axial distance, Z, conjugation parameter, β, and dimensionless distance, L, used in this work depend on the Reynolds and Prandtl numbers, comparisons are better envisioned by using the dimensionless parameters z/r_1, r_1/L^*, and $\beta\,\mathrm{Pe}^2$. Tables 1 and 2 show the results of such calculations for the cases of $0.025 \leqslant z/r_1 \leqslant 10$, $(r_1/L^*) = 0.04$, and $\beta = 100/\mathrm{Pe}^2$. The results in these tables clearly show that, for low Prandtl number, the conjugation effects become important in regions very close to the inlet. The percentage deviation of the local Nusselt number

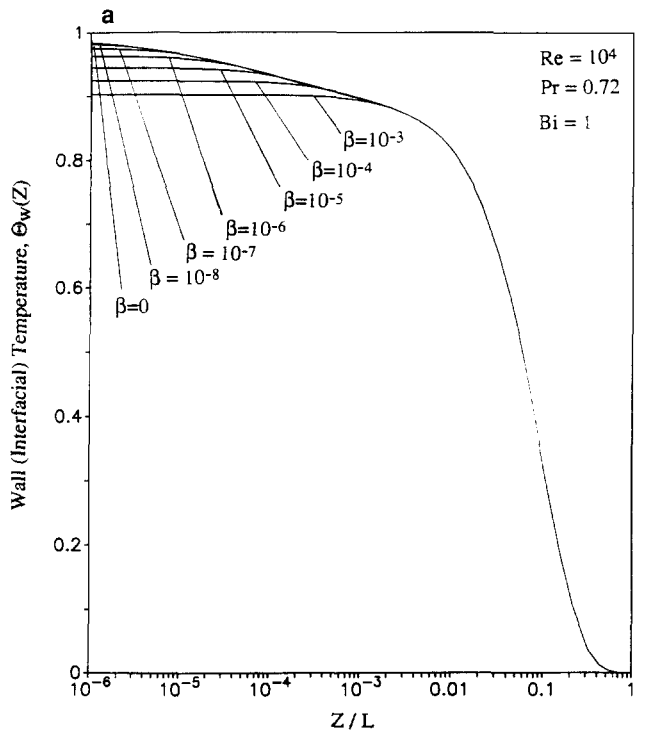

Figure 1a Effects of conjugation parameter β on temperature distribution along the wall for Bi = 1 (Pr = 0.72, Re = 10^4, $L = 10$)

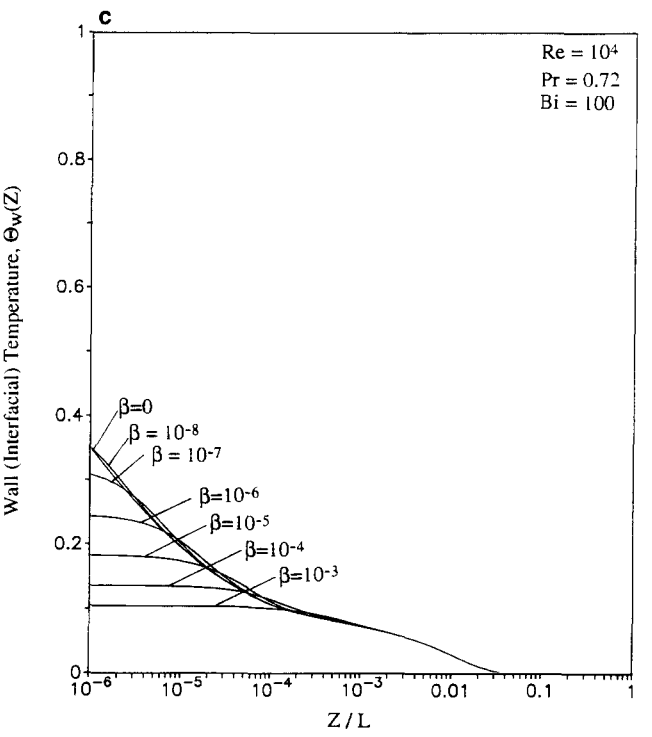

Figure 1c Effects of conjugation parameter β on temperature distribution along the wall for Bi = 100 (Pr = 0.72, Re = 10^4, $L = 10$)

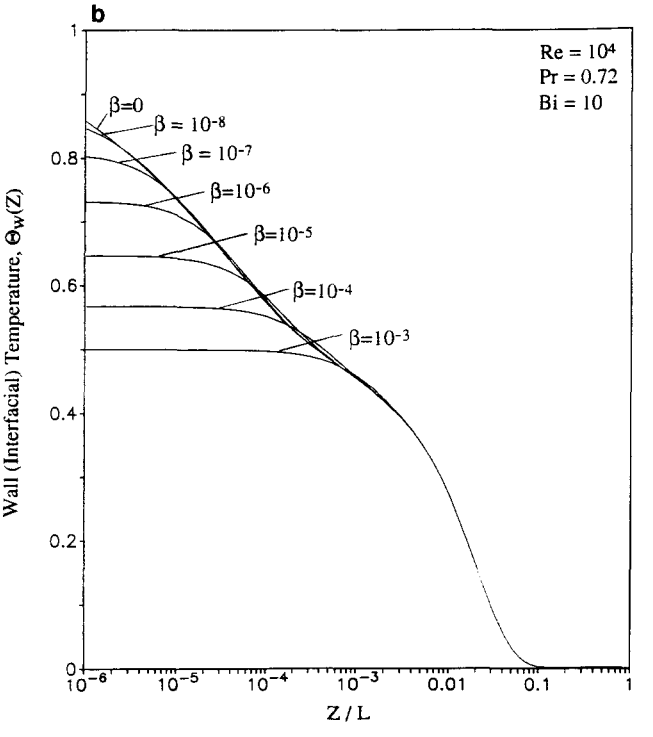

Figure 1b Effects of conjugation parameter β on temperature distribution along the wall for Bi = 10 (Pr = 0.72, Re = 10^4, $L = 10$)

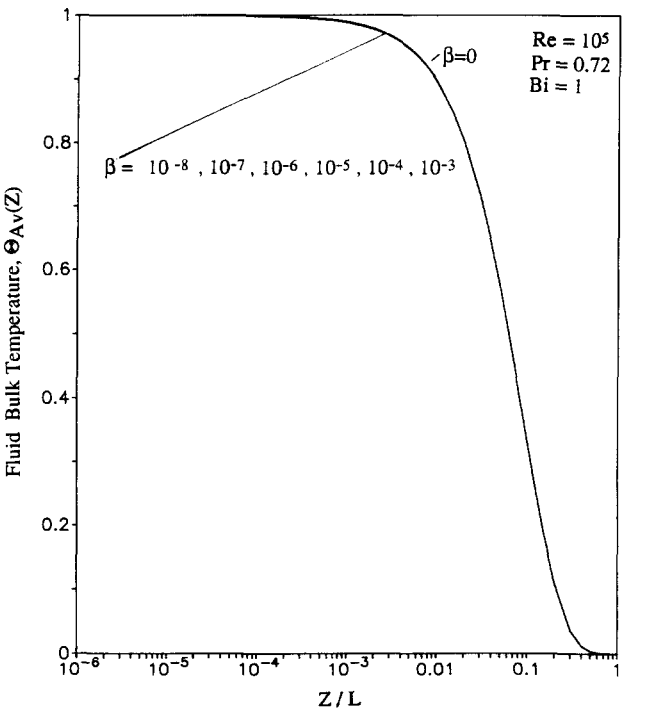

Figure 2 Fluid bulk temperature (Pr = 0.72, Re = 10^5, $L = 10$, Bi = 1, $0 \leqslant \beta \leqslant 10^{-3}$)

from that of the Graetz problem increases as Reynolds number increase from 10^4 to 10^5 for Pr = 0.01. But a similar comparison made for Pr $\geqslant$ 0.1 shows that the percentage deviation decreases instead of increasing. Such a trend was also observed by Sakakibara and Endoh (1977). For Pr > 1, the effect of wall conjugation on heat transfer is insignificant. Table 2 presents results similar to those shown in Table 1 but at a Biot number of 10 instead of 1. The same conclusions are drawn in the variation of the local Nusselt number, but the effects are reduced. Other values of r_1/L^* should not affect the conclusions above.

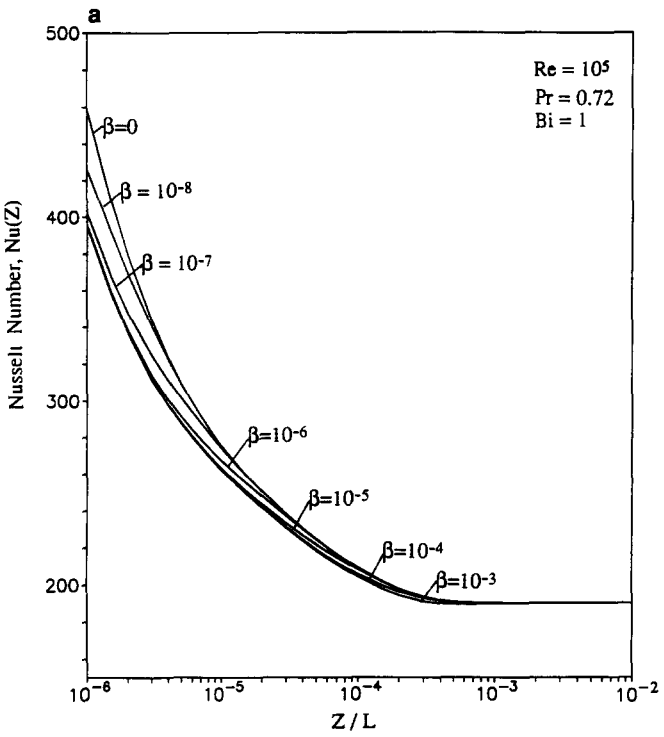

Figure 3a Local Nusselt numbers for Bi = 1 (Pr = 0.72, Re = 10^5, $L = 10$)

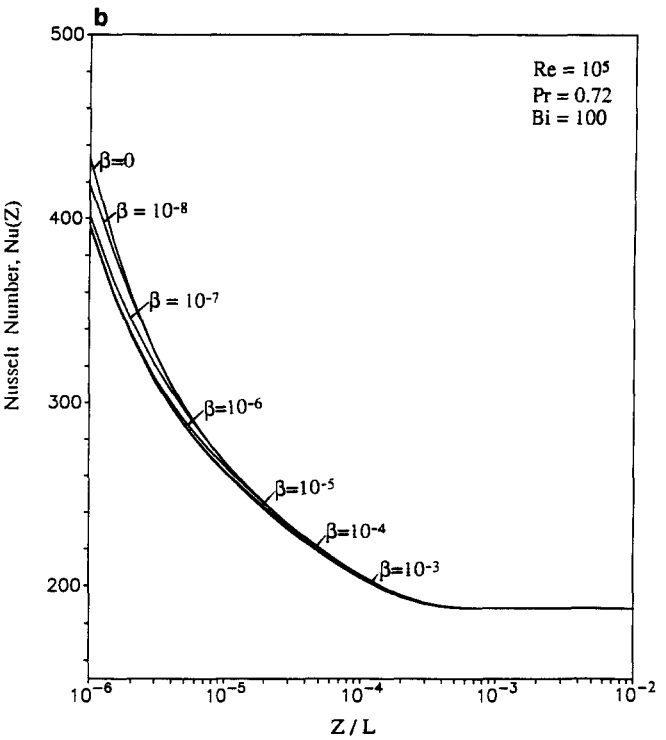

Figure 3b Local Nusselt numbers for Bi = 100 (Pr = 0.72, Re = 10^5, $L = 10$)

Table 1 Percentual deviation of the Nusselt number from the situation without wall axial conduction ($r_1/L^* = 0.04$, $\beta\,Pe^2 = 100$, Bi = 1)

		z/r_1				
Re	Pr	0.025	0.25	2.5	5.0	10.0
10^4	0.01	18.0	18.0	3.5	0.4	0.3
	0.10	16.0	15.0	2.0	0.4	0.0
	0.72	15.0	13.0	0.9	0.0	0.0
	1.00	15.0	13.0	0.8	0.0	0.0
10^5	0.01	20.0	20.0	4.0	0.0	0.0
	0.10	14.0	11.0	0.4	0.0	0.0
	0.72	13.0	7.5	0.0	0.0	0.0
	1.00	13.0	7.0	0.0	0.0	0.0

Table 2 Percentual deviation of the Nusselt number from the situation without wall axial conduction ($r_1/L^* = 0.04$, $\beta\,Pe^2 = 100$, Bi = 10)

		z/r_1				
Re	Pr	0.025	0.25	2.5	5.0	10.0
10^4	0.01	14.0	11.0	0.4	0.3	0.1
	0.10	13.7	11.0	0.2	0.1	0.0
	0.72	13.7	10.9	0.2	0.1	0.0
	1.00	13.6	10.9	0.1	0.1	0.0
10^5	0.01	17.6	16.4	0.7	0.2	0.1
	0.10	13.0	10.0	0.2	0.0	0.0
	0.72	12.0	7.0	0.1	0.0	0.0
	1.00	12.0	6.6	0.1	0.0	0.0

The present study shows that the effects of axial conduction in the wall for turbulent flow are more pronounced at low Prandtl number in regions near the inlet.

Acknowledgment

One of the authors, R. O. C. Guedes, wishes to acknowledge the financial support provided by CNPq from Brazil.

References

Barrozi, G. S. and Pagliarini, G. 1985. A method to solve conjugate heat transfer problems: the case of fully developed laminar flow in a pipe. *J. Heat Transfer ASME*, **107**, 77–83

Campo, A. and Schuler, C. 1988. Heat transfer in laminar flow through circular tubes accounting for two-dimensional wall conduction. *Int. J. Heat Mass Transfer*, **31**, 2251–2259

Cotta, R. M. and Ozisik, M. N. 1986. Transient forced convection in laminar channel flow with stepwise variations of wall temperature. *Can. J. Chem. Eng.*, **64**, 734–742

Cotta, R. M. and Ozisik, M. N. 1987. Diffusion problems with general time-dependent coefficients. *Rev. Bras. Ciencias Mecanicas*, **9**, 269–292

Faghri, M. and Sparrow, E. M. 1980. Simultaneous wall and fluid axial conduction in laminar pipe-flow heat transfer. *J. Heat Transfer ASME*, **102**, 58–63

Guedes, R. O. C., Cotta, R. M., and Brum, N. C. L. 1991. Heat transfer in laminar tube flow with wall axial conduction effects. *J. Thermophys. Heat Transfer*, **5**, 508–513

IMSL Library. 1987. *Edition 7*, GNB Building, 7500 Ballaire Blvd., Houston, Texas

von Karman, T. 1939. The analogy between fluid friction and heat transfer. *Trans. ASME*, **61**, 705–710
Kays, W. M. and Crawford, M. E. 1980. *Convective Heat and Mass Transfer*. McGraw-Hill, New York
Larson, R. I., and Yerazunis, S. 1973. Mass transfer in turbulent flow. *Int. J. Heat Mass Transfer*, **16**, 121–128
Lin, Y. K. and Chow, L. C. 1984. Effects of wall conduction on heat transfer for turbulent flow in a circular tube. *J. Heat Transfer ASME*, **106**, 597–603
Luikov, A. V., Aleksashenko, V. A., and Aleksashenko, A. A. 1971. Analytical methods of solution of conjugated problems in convective heat transfer. *Int. J. Heat Mass Transfer*, **14**, 1047–1056
Mori, S., Sakakibara, M., and Tanimoto, A. 1976. Steady heat transfer to laminar flow between parallel-plates with conduction in the wall. *Heat Transfer Jpn. Res.*, **5**, 17–25
Notter, R. H. and Sleicher, C. A. 1972. A solution to the turbulent Graetz problem—III. Fully developed and entry region heat transfer rates. *Chem. Eng. Sci.*, **27**, 2073–2093
Ozisik, M. N. and Murray, R. L. 1974. On the solution of linear diffusion problems with variable boundary condition parameters. *J. Heat Transfer ASME*, **96**, 48–51
Ozisik, M. N., Cotta, R. M., and Kim, W. S. 1989. Heat transfer in turbulent forced convection between parallel-plates. *Can. J. Chem. Eng.*, **67**, 771–776
Reichardt, H. 1951. Vollstandige Darstellung der turbulenten Geschwindigkeits-verteilung in glatten Leitungen. *Z. Angew. Math. Mech.*, **31**, 208–219
Sakakibara, M. and Endoh, K. 1977. Effect of conduction in wall on heat transfer with turbulent flow between parallel-plates. *Int. J. Heat Mass Transfer*, **20**, 507–516
Shah, R. K. and London, A. L. 1978. Laminar flow forced convection in ducts. In *Advances in Heat Transfer*. Academic Press, New York.
Shah, R. K. and Bhatti, M. S. 1987. Laminar convective heat transfer in ducts. In *Handbook of Single-Phase Convective Heat Transfer*, Kakac, S., Shah, R. K., and Aung, W. (eds.). John Wiley, New York.
Spalding, D. B. 1961. Heat transfer to a turbulent stream from a surface with a step-wise discontinuity in wall temperature. *Conf. Intern. Dev. Heat Transfer ASME*, Boulder, CO, part 2, 439–446
Wijeysundera, N. E. 1986. Laminar forced convection in circular and flat ducts with axial conduction and external convection. *Int. J. Heat Mass Transfer*, **29**, 797–807
Yan, W. M., Fin, T. F., and Lee, T. L. 1990. Steady conjugate heat transfer in turbulent channel flows. *Warme- und Stoffubertragung*, **25**, 215–220
Zariffeh, E. K., Soliman, N. M., and Trupp, A. C. 1982. The combined effects of wall and fluid axial conduction on laminar heat transfer in circular tubes. *Proc. 7th International Heat Transfer Conf.*, **3**, München, Germany, pp. 131–136

Appendix 1

The three-layer turbulent velocity distribution is taken as follows: Laminar sublayer (Spalding 1961; von Karman 1939):

$$u^+ = r^+ \quad \text{for} \quad 0 \leqslant r^+ \leqslant 5$$

Buffer layer (Spalding 1961; von Karman 1939):

$$u^+ = -3.05 + 5 \ln r^+ \quad \text{for} \quad 5 \leqslant r^+ \leqslant 30$$

Turbulent core (Reichardt 1951; Kays and Crawford 1980):

$$u^+ = 5.5 + 2.5 \ln\left[r^+ \frac{1.5(1+R)}{1+2R^2} \right] \quad \text{for} \quad r^+ > 30$$

The momentum eddy diffusivity is taken as follows (Spalding 1961):

$$\frac{\varepsilon_m}{\nu} = \frac{k}{E}\left[e^{ku^+} - 1 - ku^+ - \frac{(ku^+)^2}{2!} - \frac{(ku^+)^3}{3!} \right] \quad \text{for} \quad r^+ < 40$$

where $k = 0.407$ and $E = 10$, and (Reichardt 1951)

$$\frac{\varepsilon_m}{\nu} = \frac{kR^+}{6}(1 - R^2)(1 + 2R^2) \quad \text{for} \quad r^+ \geqslant 40$$

where

$$k = 0.4, \quad R^+ = \frac{\mathrm{Re}}{4}\sqrt{\frac{f_m}{8}}, \quad r^+ = (1 - R)R^+, \quad u^+ = \frac{u}{\bar{u}\sqrt{\frac{f_m}{8}}},$$

and

$$R = r/r_1$$

The turbulent Prandtl number $\mathrm{Pr}_t (= \varepsilon_m/\varepsilon_h)$ is taken as

$$\mathrm{Pr}\,\frac{35 + (\varepsilon_m/\nu)}{[0.025\,\mathrm{Pr}(\varepsilon_m/\nu) + 90\,\mathrm{Pr}^{3/2}(\varepsilon_m/\nu)^{1/4}][45 + (\varepsilon_m/\nu)]}$$

for $\mathrm{Pr} = 0.01$ and 0.1 (Notter and Sleicher 1972), and $\mathrm{Pr}_t = 0.86$ for $\mathrm{Pr} = 0.72$ (Larson and Yerazunis 1973).

Appendix 2: Determination of C

The velocity ratio $C = u_{max}/\bar{u}$ is expressed as

$$C = u^+_{max}\sqrt{\frac{f_m}{8}}$$

where

$$u^+_{max} = 5.5 + 2.5 \ln(1.5R^+).$$

Therefore, for a given Reynolds number Re and friction factor f_m, C is readily determined from these expressions.

Appendix 3: Determination of friction factor f_m

The relation between Reynolds number $\mathrm{Re} = \bar{u}D_e/\nu$ and R^+ is given by

$$\frac{\mathrm{Re}}{4} = \int_0^{R^+} u^+ \, dr^+ \tag{A1}$$

which can be transformed as

$$\sqrt{\frac{f_m}{8}}\int_0^1 u^+(R)\, dR \tag{A2}$$

For a given Reynolds number, Equation A2 provides a transcendental equation for the determination of f_m.